Table III. Selected Atomic Distances (Å) for the Anion $[Mo_2Cu_5S_8(S_2CNMe_2)]^{2-}$

Mo(1)–Cu(1)	2.636 (1)	Mo(2)–Cu(3)	2.664 (2)
Mo(2)–Cu(2)	2.725 (1)	Cu(1)–Cu(2)	2.765 (2)
Cu(1)–Cu(1)′	3.495 (1)	Cu(2)–Cu(3)	3.703 (2)
Cu(2)–Cu(2)′	3.762 (1)		
Mo(1)–S(1)	1.942 (7)	Mo(2)–S(4)	2.123 (4)
Mo(1)–S(2)	2.289 (4)	Mo(2)–S(5)	2.273 (3)
Mo(1)–S(3)	2.229 (2)	Mo(2)–S(6)	2.235 (2)
Cu(1)–S(2)	2.231 (2)	Cu(2)–S(12)	2.265 (3)
Cu(1)–S(3)	2.251 (3)	Cu(2)–S(3)	2.495 (3)
Cu(1)–S(11)	2.189 (3)	Cu(3)–S(6)	2.266 (3)
Cu(2)–S(5)	2.300 (2)	Cu(3)–S(21)	2.360 (4)
Cu(2)–S(6)	2.301 (3)	Cu(3)–S(22)	2.430 (4)

Table IV. Selected Bond Angles (deg) for the Anion $[Mo_2Cu_5S_8(S_2CNMe_2)_3]^{2-}$

S(1)–Mo(1)–S(2)	109.7 (3)	S(4)–Mo(2)–S(5)	114.0 (2)
S(1)–Mo(1)–S(3)	111.2 (1)	S(4)–Mo(2)–S(6)	109.1 (1)
S(2)–Mo(1)–S(3)	107.6 (1)	S(5)–Mo(2)–S(6)	108.1 (1)
S(3)–Mo(1)–S(3)′	109.6 (1)	S(6)–Mo(2)–S(6)′	108.5 (1)
S(2)–Cu(1)–S(3)	108.8 (1)	S(5)–Cu(2)–S(12)	127.0 (1)
S(2)–Cu(1)–S(11)	120.2 (1)	S(6)–Cu(2)–S(12)	104.5 (2)
S(3)–Cu(1)–S(11)	129.0 (1)	S(6)–Cu(3)–S(21)	121.3 (1)
S(3)–Cu(2)–S(5)	114.2 (2)	S(6)–Cu(3)–S(22)	115.3 (1)
S(3)–Cu(2)–S(6)	102.3 (1)	S(6)–Cu(3)–S(6)′	106.3 (1)
S(3)–Cu(2)–S(12)	101.3 (1)	S(21)–Cu(3)–S(22)	74.6 (1)
S(5)–Cu(2)–S(6)	105.0 (2)		
Mo(1)–S(2)–Cu(1)	71.3 (1)	Mo(2)–S(5)–Cu(2)	73.2 (1)
Cu(1)–S(2)–Cu(1)	103.1 (1)	Cu(2)–S(5)–Cu(2)	109.8 (2)
Mo(1)–S(3)–Cu(1)	72.1 (1)	Mo(2)–S(6)–Cu(2)	73.8 (1)
Mo(1)–S(3)–Cu(2)	113.8 (1)	Mo(2)–S(6)–Cu(3)	72.6 (1)
Cu(1)–S(3)–Cu(2)	71.1 (1)	Cu(2)–S(6)–Cu(3)	108.3 (1)
Cu(1)–S(11)–C(11)	106.8 (3)	Cu(3)–S(21)–C(21)	85.0 (5)
Cu(2)–S(12)–C(11)	114.5 (3)	Cu(3)–S(22)–C(21)	82.5 (5)

found and collected. This was washed with 1:4 (v/v) DMF–THF and dried in vacuo to afford 1.5 g (35%) of product. The IR spectrum (KBr) shows a characteristic $Mo{=}S_t$ absorption at 513 cm^{-1} and $Mo–S_b$ absorptions at 455, 444, and 422 cm^{-1}. Anal. calcd for $C_{25}H_{62}Cu_5Mo_2N_5O_2S_{14}$: C, 21.10; H, 4.40; Cu, 22.32; Mo, 13.48; N, 4.92; S, 31.54. Found: C, 20.62; H, 4.93; Cu, 21.62; Mo, 13.25; N, 4.93; S, 30.54. Elemental analyses were performed by the Analytical Chemistry Group of this institute.

Instrumentation. Proton NMR spectra were recorded on a Varian FT-80A spectrometer. DMSO-d_6 was used as solvent and TMS as internal standard with positive values given to downfield shifts. IR spectra were recorded on a Digilab-20E/D spectrophotometer.

Structure Determination. Diffraction data for the title compound were collected at room temperature on an Enraf-Nonius CAD4 diffractometer using graphite-monochromatized Mo Kα radiation (λ = 0.71073 Å). The single crystal of the title compound was kept from air by a coating of epoxy resin. An empirical absorption correction (ψ scan) was applied. After data reduction (including correction for Lorentz and polarization effects), the remaining unique reflections with $I > 3\sigma(I)$ were used for the subsequent structure solution and refinement. Calculations were performed on a VAX 11/785 computer with the SDP program package. All metal atoms were located from an E map. A Fourier map phased by the metal atoms contained most of the remaining non-hydrogen atoms. Full-matrix least-squares refinement with anisotropic thermal parameters for all non-hydrogen atoms except oxygen atoms led to convergence. Crystallographic data appear in Table I, and the atomic coordinates and thermal parameters are listed in Table II.

Results and Discussion

Since there are four formula units per unit cell and eight general positions, each $[Mo_2Cu_5S_8(S_2CNMe_2)_3]^{2-}$ anion is situated about a crystallographic mirror plane: atoms Mo(1), Mo(2), Cu(3), S(1), S(2), S(4), and S(5) are located on the mirror plane. The structure of the anion is depicted in Figure 1. Another view is shown in Figure 2. The $Mo_2Cu_5S_8$ framework consists of the two cubane-like units $[SMoS_3Cu_2]$ (I) and $[SMoS_3Cu_3]$ (II). These two units are similar to the cores in the compounds $[OMoS_3(CuPPh_3)Cu(PPh_3)_2]$ and $[OMoS_3(CuCl)_3]^{2-}$, respectively.[5] They are linked through two weak Cu–S bonds (Cu(2)–S(3) and Cu(2)′–S(3)′ = 2.495 (3) Å), and the two sets of copper atoms Cu(1)–Cu(2) and Cu(1)′–Cu(2)′ are connected by bridging Me_2dtc ligands. Tables III and IV list the main atomic distances and main bond angles, respectively.

Structure analysis shows that each of the two molybdenum atoms is in an S_4 tetrahedral center. The average bond angle of S–Mo–S for both units is 109.7 (20)°. However, the values of Mo–S distances vary, with the terminal Mo–S bond as the shortest, i.e. 1.942 (7) and 2.123 (4) Å in units I and II, respectively. From a structural point of view, there are three kinds of Cu atoms in this molecule: (a) atoms Cu(1) and Cu(1)′ are essentially in the center of the trigonal planes of S(2), S(3), S(11) and S(2), S(3)′, S(11)′, respectively; (b) atoms Cu(2) and Cu(2)′ are each in a slightly distorted tetrahedral environment; (c) atom Cu(3) is in the center of a highly distorted tetrahedron of atoms S(6), S(6)′, S(21), and S(22) with an angle S(21)–Cu(3)–S(22) of 74.6 (1)°, which is a normal chelate angle for $M(R_2dtc)$. Each of the six bridging sulfur atoms is triply connected. The three Me_2dtc ligands are of two types: two of these are bridging ligands connecting two copper atoms, Cu(1)–Cu(2) and Cu(1)′–Cu(2)′; the third is a terminal ligand chelating to atom Cu(3).

The title compound is diamagnetic from the magnetic susceptibility measurement. The ^1H NMR signal of $CH_3–$ in Me_2dtc exhibits no paramagnetic broadening. The chemical shifts of $–N(CH_3)_2$ in all three Me_2dtc ligands are 3.5 ppm in DMSO-d_6 at room temperature.

The fact that the IR spectrum of the title compound is more complicated than that of $[MoS_4Cu_3(R_2dtc)_3]^{2-}$[8] in the region of 400–500 cm^{-1} is an indication of several different $Mo–S_b$ absorptions. The absorption at 513 cm^{-1} is a characteristic stretching of the terminal $Mo{=}S_t$ bond.

Acknowledgment. This work was supported by a National Natural Science Foundation Grant and by a Provincial Science Fund of Fujian.

Supplementary Material Available: A listing of the crystallographic data, full listings of atomic distances and bond angles, a listing of anisotropic thermal parameters, a view of the packing scheme in the unit cell, and an IR spectrum (6 pages); a listing of calculated and observed structure factors (15 pages). Ordering information is given on any current masthead page.

Contribution from the Departments of Chemistry,
Lanzhou University, Lanzhou Gansu, PRC,
and Northwestern University, Evanston, Illinois 60208

Kinetics and Mechanism of Carbon Monoxide Substitution of Osmium Pentacarbonyl

Jian-Kun Shen,[†] Yi-Ci Gao,[†] Qi-Zhen Shi,[*,†] and Fred Basolo[*,‡]

Received February 24, 1989

Although osmium pentacarbonyl has been known[1] for more than four decades, no kinetic data have been reported on its rate of carbon monoxide substitution. With reference to early observations[2] that for a given transition-metal triad the organometallic complexes of the second-row metals are the most substitution labile, it is of interest to compare the rates of CO substitutions of the carbonyls $M(CO)_5$ (M = Fe, Ru, Os). Kinetic data are available for the rate of CO exchange of $Fe(CO)_5$,[3] for CO

[†] Lanzhou University.

[‡] Northwestern University.

0020-1669/89/1328-4304$01.50/0

Table I. Rate Constants for the Reaction in Decalin[a]

$$Os(CO)_5 + L \rightarrow Os(CO)_4L + CO$$

T, °C	L	10^2[L], M	10^5k_{obs}, s^{-1}
96.0	PPh_3	1.87	1.11
		3.73	0.93
		11.2	1.10
86.0	PPh_3	3.73	0.32
		7.46	0.34
	$P(n\text{-}Bu)_3$	3.35	0.31
		6.70	0.32
76.4	PPh_3	3.35	0.10

[a] $\Delta H^* = 30.6 \pm 0.3$ kcal/mol. $\Delta S^* = 1.33 \pm 0.03$ cal/(mol K).

substitution of $Fe(CO)_4PPh_3$,[4] and for CO substitution of $Ru(CO)_5$.[5] This note reports kinetic data for the CO substitution of $Os(CO)_5$, which allows a comparison of ligand substitution lability for this triad of binary metal carbonyls.

Experimental Section

Chemical Compounds. $Os(CO)_5$ was provided by Professor Josef Takats and Dr. Gong-Yu Kiel. PPh_3 was purified by recrystallization from anhydrous ethyl alcohol. $P(n\text{-}Bu)_3$ was purified by distillation under a N_2 atmosphere. Decalin was dehydrated with Na and distilled under a N_2 atmosphere before use.

Kinetic Procedure. Solutions for the study of substitution reactions were degassed by three freeze–pump–thaw cycles. All the reactions were followed with a Nicolet 7199 FT-IR spectrophotometer using a 0.2-mm NaCl cell. All the reactions were carried out in Schlenk tubes sealed with rubber septum caps, through which the samples were taken with a syringe. Because the volatility of $Os(CO)_5$ at the temperatures used is a problem, small schlenk tubes were used almost completely filled with reaction solution. This means there is a negligible amount of $Os(CO)_5$ and no condensation of liquid on the hot walls of the Schlenk tube. Rate data were obtained by following the disappearance of the CO stretching band of $Os(CO)_5$ at 1993 cm^{-1} and using eq 1 for calculations.

$$\ln A_t = -k_{obsd}t + \text{constant} \quad (1)$$

Results

The CO substitution reaction (eq 2) was carried out in decalin solution, under a N_2 atmosphere, between 76 and 96 °C, and in the absence of light. At much higher temperatures, because of

$$\begin{gathered} Os(CO)_5 + L \rightarrow Os(CO)_4L + CO \\ L = PPh_3,\ P(n\text{-}Bu)_3 \end{gathered} \quad (2)$$

the $Os(CO)_5$ volatility, the correlation coefficients of k_{obsd} were not good enough to give reliable rate constants. With the experimental precaution noted above, the rate constants were reproducible to better than 10%. The rates of reaction (eq 2) are first order in $Os(CO)_5$ concentration and zero order in L concentration (Table I). The correlation coefficients of k_{obsd} values in Table I are all above 0.998 for 2 half-lives of the reaction. Even after 4 half-lives there is no spectroscopic evidence for the formation of $Os(CO)_3L_2$. The monosubstituted products, $Os(CO)_4L$, had IR spectra in good agreement with the literature.[6]

Discussion

A first-order rate law for the reaction (eq 2) is consistent with the usual dissociative mechanism for substitution reactions of 18-electron binary metal carbonyls.[7] Also in support of a dissociative mechanism is the large value of ΔH^* (Table I), which is generally observed for processes where metal–ligand bond breaking dominates the energetics of the rate-determining process. Usually the positive value of ΔS^* is larger than that observed (Table I), indicating perhaps the Os–CO bond is not completely broken in the transition state for the reaction. However, the contribution made to the total reaction energetics by the entering ligand is not experimentally detectable, because the rates are zero order in PPh_3 and in $P(n\text{-}Bu)_3$ concentrations. In the absence of phosphine and under the conditions of these experiments, the mononuclear osmium carbonyl trimerizes. Thus the overall reaction process may be designated as

Table II. Rate Constant and Activation Parameters for CO Substitution of Metal Carbonyls

complex	k, s^{-1} [a]	ΔH^*, kcal/mol	ΔS^*, cal/(mol K)
$Fe(CO)_5$[b]	6×10^{-11}	40	18
$Fe(CO)_4PPh_3$[c]	1.27×10^{-12}	42.5 ± 1.2	18.4 ± 2.8
$Ru(CO)_5$[d]	3.0×10^{-3}	27.6 ± 0.40	15.2 ± 1.3
$Ru(CO)_4PPh_3$[e]	1.78×10^{-4}	30.1	17.3
$Os(CO)_5$	4.9×10^{-8}	30.6 ± 0.3	1.33 ± 0.03
$Fe_3(CO)_{12}$[f]	9.84×10^{-4}	29.1 ± 1.5	17.6 ± 5.0
$Ru_3(CO)_{12}$[f]	1.02×10^{-4}	32.2 ± 1.7	22.7 ± 3.7
$Os_3(CO)_{12}$[f]	1.03×10^{-8}	33.7 ± 1.5	10.7 ± 4.1

[a] At 50 °C; calculated values. [b] Estimates are made by assuming the introduction of PPh_3 into $Fe(CO)_5$ increases ΔH^* values by 30.1 − 27.6 = 2.5 kcal/mol (using ΔH^* values for corresponding Ru compounds); then the value of ΔH^* for $Fe(CO)_5$ is 42.5 − 2.5 = 40 kcal/mol. Further, assuming the ΔS^* values for reactions of $Fe(CO)_5$ and $Fe(CO)_4PPh_3$ are about the same, then k_1 (50 °C) for $Fe(CO)_5$ is estimated to be 6×10^{-11} s^{-1}. [c] Reference 4. [d] Reference 5. [e] Reference 8. [f] Reference 16.

$$\begin{tikzcd} Os(CO)_5 \arrow[r, "-CO"] & \text{"}Os(CO)_4\text{"} \arrow[r, "+L"] \arrow[d] & Os(CO)_4L \\ & Os_3(CO)_{12} & \end{tikzcd}$$

It would be of interest to compare the rate of trimerization with that of $Os(CO)_4L$ formation, but unfortunately the solution becomes cloudy upon trimerization and rate data were not obtained.

Previous studies[3-5] show that the other members of this carbonyl triad ($Fe(CO)_5$ and $Ru(CO)_5$) also undergo CO substitution by a dissociation mechanism. The rate of CO substitution of $Fe(CO)_5$ has not been determined, because of its high volatility and low stability at the extremely high temperatures required for its reaction.[4] However, it has been estimated[3] that $Fe(CO)_5$ has a rate of exchange with ^{14}CO at 25 °C with a half-life greater than 4 years. The rate of CO substitution of the less volatile $Fe(CO)_4PPh_3$ to give $Fe(CO)_3(PPh_3)_2$ was reported.[4] If it is assumed that the difference in rates of CO substitution between $Fe(CO)_5$ and $Fe(CO)_4PPh_3$ is about the same as that between $Ru(CO)_5$[5] and $Ru(CO)_4PPh_3$,[8] then one can approximate a rate for $Fe(CO)_5$ (Table II).

This estimate of the rate of CO substitution for $Fe(CO)_5$, along with our determination of the rate of reaction (eq 2) of $Os(CO)_5$ and the literature[5] value of the rate for $Ru(CO)_5$, allows one to compare the substitution reactivities of $M(CO)_5$ (M = Fe, Ru, Os). Reactivities increase in the order Fe < Os < Ru, which is yet another example of the second-row metal of organometallic complexes reacting the fastest.[2] It is now well-known[9] that generally homogeneous catalyses of transition-metal organometallic compounds involve compounds of second-row transition metals.

The observation, made in the 1960s, that such second-row transition-metal complexes are the most substitution labile of a given triad of metals has been explained in different ways over the years and continues to be explained in more sophisticated language. An early attempt to account for the behavior suggested[10] stabilization of the M–CO bond for the first-row metal

---

(1) Heiber, W.; Stallmann, H. *Z. Elektrochem.* **1943**, *49*, 288.

(2) (a) Basolo, F.; Pearson, R. G. *Mechanisms of Inorganic Reactions*, 2nd ed.; Wiley: New York, 1967; p 576. (b) Pajaro, G.; Calderazzo, F.; Ercoli, R. *Gazz. Chim. Ital.* **1960**, *90*, 1486. (c) Cetini, G.; Gambino, O. *Atti Accad. Sci. Torino, Cl. Sci. Fis., Mat. Nat.* **1963**, *97*, 757, 1189, 1197. (d) Shuster-Woldan, H. G.; Basolo, F. *J. Am. Chem. Soc.* **1966**, *88*, 1657.

(3) Keeley, D. F.; Johnson, R. E. *J. Inorg. Nucl. Chem.* **1959**, *11*, 33.

(4) Siefert, E. E.; Angelici, R. J. *J. Organomet. Chem.* **1967**, *8*, 374.

(5) Huq, R.; Poë, A. J.; Chawla, S. *Inorg. Chim. Acta* **1980**, *38*, 121.

(6) L'Epplattenir, F.; Calderazzo, F. *Inorg. Chem.* **1968**, *7*, 1290.

(7) Howell, J. A. S; Burkinshaw, P. M. *Chem. Rev.* **1983**, *83*, 557.

(8) Johnson, B. F. G.; Lewis, J.; Twigg, M. V. *J. Chem. Soc., Dalton Trans.* **1975**, 1876.

(9) Parshall, G. W. *Homogeneous Catalysis*; Wiley: New York, 1980. Basolo, F. *Isr. J. Chem.* **1986**, *27*, 233.

(10) Meier, M.; Basolo, F.; Pearson, R. G. *Inorg. Chem.* **1969**, *8*, 795.

by predominately π bonding and the third-row metal system by largely σ bonding, thus leaving the second-row metal complex to be the most labile. A similar explanation[11] is given in terms of the low electronegativity of the metal of the first transition series as one factor and a good matching of the orbital energies of the third-transition-series metal with those of the CO ligand as the second factor. The latest word[12] on this, to our knowledge, is the detailed molecular orbital calculations based on density functional theory to estimate the first CO ligand dissociation energy ΔH of $M(CO)_m$ for the three binary metal carbonyl triads $M(CO)_6$ (M = Cr, Mo, W), $M(CO)_5$ (M = Fe, Ru, Os), and $M(CO)_4$ (M = Ni, Pd, Pt). For each triad of transition metals, the calculated ordering of the M–CO bond strength (including relativistic effects) is 3d > 5d > 4d. These calculations agree with the experimental observation that second-row (4d) transition metals generally afford the most substitution labile organometallic complexes of a given metal triad.

The anomaly for the $M(CO)_5$ (M = Fe, Ru, Os) triad is the extreme slowness of CO substitution of iron pentacarbonyl relative to the pentacarbonyls of ruthenium and osmium. The reason for this perhaps rests largely in the fact that the transition state/active intermediate for reaction, $Fe(CO)_4$, may be high spin.[13] Thus, a partial explanation for this very slow rate of CO substitution of $Fe(CO)_5$ may be the much less favorable crystal field activation energy (CFAE)[14] in going from low-spin $Fe(CO)_5$ to high-spin $Fe(CO)_4$, compared with the CFAE in going from low-spin $M(CO)_5$ (M = Ru, Os) to low-spin $M(CO)_4$.[15] The electron spin change for $Fe(CO)_5$ corresponds to a spin-forbidden process, whereas that for $Ru(CO)_5$ and $Os(CO)_5$ should involve a spin-allowed process. This spin change for $Fe(CO)_5$ makes its formation of triplet $Fe(CO)_4$ a slower process than formation of a singlet transition state, so its reaction may involve the less stable singlet $Fe(CO)_4$.

Although the enthalpy of activation (ΔH^*) for CO substitution of $Os(CO)_5$ is about 3 kcal/mol less than for $Os_3(CO)_{12}$,[16] the rate constants at 50 °C for the two reactions are almost the same (Table II). This results from the much smaller value of ΔS^* for the mononuclear metal carbonyl compared to that for the cluster. The rates of CO substitution of the mononuclear and cluster ruthenium carbonyls are also almost the same at 50 °C, but $Fe_3(CO)_{12}$ reacts much faster than does $Fe(CO)_5$ (Table II). As already discussed, the slow reaction of $Fe(CO)_5$ may be associated with its spin change from low spin in the ground state to high spin in the transition state. Also, the greater ease with which the iron cluster $Fe_3(CO)_{12}$ forms bridging COs is believed,[17] in part, to be the reason it reacts faster than do the corresponding ruthenium and osmium clusters.

Acknowledgment. We thank the USA-PRC Cooperative Science Program for the support of this collaborative research. The program is funded by the U.S. National Science Foundation and by the PRC National Natural Science Foundation. Additonal support was provided by NSF Grant CHE-8818696. We are grateful to Professor Josef Takats and Dr. Gong-Yu Kiel for a gift of $Os(CO)_5$ and to Dr. Paula Bogdan for its procurement.

Registry No. $Os(CO)_5$, 16406-49-8; PPh_3, 603-35-0; PBu_3, 998-40-3.

---

[11] Beach, N. A.; Gray, H. B. *J. Am. Chem. Soc.* **1968**, *90*, 5713.

[12] Ziegler, T.; Tschinke, V.; Ursenbach, C. *J. Am. Chem. Soc.* **1987**, *109*, 4825.

[13] Burdett, J. K. *J. Chem. Soc., Faraday Trans. 2* **1974**, *70*, 1599. Poliakoff, M.; Turner, J. J. *J. Chem. Soc., Dalton Trans.* **1974**, 2276.

[14] Reference 2, pp. 145–158. Modi, S. P.; Atwood, J. D. *Inorg. Chem.* **1983**, *22*, 26.

[15] Ziegler, T. *Inorg. Chem.* **1986**, *25*, 2721.

[16] Candlin, J. P.; Shortland, A. C. *J. Organomet. Chem.* **1969**, *16*, 289. Shojaie, A.; Atwood, J. D. *Organometallics* **1985**, *4*, 187. Poë, A. J.; Sekhar, V. C. *Inorg. Chem.* **1985**, *24*, 4377.

[17] Sonnenberger, D.; Atwood, J. D. *J. Am. Chem. Soc.* **1980**, *102*, 3484.

Additions and Corrections

1989, Volume 28

Thomas C. Strekas,* Harry D. Gafney, Steven A. Tysoe, Randolph P. Thummel,* and Francois Lefoulon: Resonance Raman Spectra and Excited-State Lifetimes for a Series of 3,3′-Polymethylene-2,2′-bipyridine Complexes of Ruthenium(II).

Page 2965. The structure near the top of column 1 was incorrectly reproduced, omitting the 2,2′-bond. The correct structure is given below:

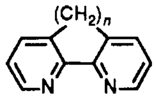

1a, $n = 1$
b, $n = 2$
c, $n = 3$
d, $n = 4$

—Thomas C. Strekas